

A NEW PARALLAX MEASUREMENT FOR THE COLDEST KNOWN BROWN DWARF<sup>1</sup>K. L. LUHMAN<sup>2,3</sup> AND T. L. ESPLIN<sup>2</sup>*Draft version July 16, 2018*

## ABSTRACT

WISE J085510.83–071442.5 was recently discovered as the coldest known brown dwarf based on four epochs of images from the *Wide-field Infrared Survey Explorer* and the *Spitzer Space Telescope*. We have improved the accuracy of its parallax measurement by obtaining two additional epochs of *Spitzer* astrometry. We derive a parallactic distance of  $2.31 \pm 0.08$  pc, which continues to support its rank as the fourth closest known system to the Sun when compared to WISE J104915.57–531906.1 AB ( $2.02 \pm 0.02$  pc) and Wolf 359 ( $2.386 \pm 0.012$  pc). The new constraint on the absolute magnitude at  $4.5 \mu\text{m}$  indicates an effective temperature of 235–260 K based on four sets of theoretical models. We also show the updated positions of WISE J085510.83–071442.5 in two color-magnitude diagrams. Whereas Faherty and coworkers cited its location in  $M_{W2}$  versus  $J - W2$  as evidence of water clouds, we find that those data can be explained instead by cloudless models that employ non-equilibrium chemistry.

*Subject headings:* brown dwarfs — infrared: stars — proper motions — solar neighborhood — stars: low-mass

## 1. INTRODUCTION

Distance is a key parameter in characterizing the physical properties of brown dwarfs and testing models of their atmospheres and interiors. A distance estimate enables the measurement of absolute magnitudes in various photometric bands. The spectral energy distribution constructed from those magnitudes can be compared to theoretical predictions in order to derive stellar parameters like mass and effective temperature and to discriminate among competing models. Distances of nearby L and T dwarfs have been measured via trigonometric parallaxes through imaging at red optical and near-infrared (IR) wavelengths (Dahn et al. 2002; Tinney et al. 2003; Vrba et al. 2004; Marocco et al. 2010; Andrei et al. 2011; Faherty et al. 2012; Dupuy & Liu 2012; Manjavacas et al. 2013; Smart et al. 2013; Wang et al. 2014; Zapatero Osorio et al. 2014). Because near- to mid-IR colors become rapidly redder toward the end of the T spectral sequence (Kirkpatrick et al. 2011), parallaxes of late-T and Y dwarfs (Tinney et al. 2012; Beichman et al. 2013, 2014; Dupuy & Kraus 2013; Marsh et al. 2013) have required the most sensitive near-IR cameras that are available, namely those on 8–10 m ground-based telescopes and the *Hubble Space Telescope*, or the mid-IR cameras on the *Wide-field Infrared Survey Explorer* (WISE, Wright et al. 2010) and the *Spitzer Space Telescope* (Werner et al. 2004).

WISE J085510.83–071442.5 (hereafter WISE 0855–0714) is a recently discovered brown dwarf for which a parallax measurement has had important implications. It was identified as a high proper motion object by Luhman (2014a) based on two epochs of

images from WISE<sup>4</sup>. By obtaining two additional epochs of astrometry with *Spitzer*, Luhman (2014b) confirmed its large proper motion and measured its parallax. The parallactic distance of  $2.20^{+0.24}_{-0.20}$  pc was roughly midway between the distances of the third and fourth closest neighbors that were previously known, WISE J104915.57–531906.1 AB ( $2.02 \pm 0.02$  pc, Luhman 2013; Boffin et al. 2014) and Wolf 359 ( $2.386 \pm 0.012$  pc, Wolf 1919; van Altena et al. 1995). Based on its absolute magnitude at  $4.5 \mu\text{m}$  and its  $[3.6] - [4.5]$  color, Luhman (2014b) also found that WISE 0855–0714 was the coldest known brown dwarf ( $T_{\text{eff}} \sim 225\text{--}260$  K). Wright et al. (2014) measured a fifth epoch of astrometry with the reactivated WISE satellite (*NEOWISE*, Mainzer et al. 2014) and derived new estimates of the proper motion and parallax. In this paper, we present two new epochs of *Spitzer* astrometry for WISE 0855–0714, which are used to improve the accuracy of its parallax measurement.

## 2. SPITZER ASTROMETRY

Luhman (2014b) obtained images of WISE 0855–0714 with *Spitzer*'s Infrared Array Camera (IRAC; Fazio et al. 2004) on 2013 June 21 and 2014 January 20. To further refine its parallax measurement, we observed WISE 0855–0714 with IRAC on two additional dates, February 24 and July 1 in 2014. These observations were performed through Astronomical Observation Requests 49096192 and 51040000 within programs 90095 and 10168, respectively. IRAC currently operates with filters centered at  $3.6$  and  $4.5 \mu\text{m}$ , which are denoted as  $[3.6]$  and  $[4.5]$ . Only the  $[4.5]$  filter was selected for our imaging because it offers much better sensitivity to cold brown dwarfs. The camera has a plate scale of  $1''.2 \text{ pixel}^{-1}$  and a field of view of  $5''.2 \times 5''.2$ . It produces images with FWHM =  $1''.7$ . The exposure time for the individual frames was 26.8 s. Five and nine dithered frames

<sup>1</sup> Based on observations made with the *Spitzer Space Telescope*, which is operated by the Jet Propulsion Laboratory, California Institute of Technology under a contract with NASA.

<sup>2</sup> Department of Astronomy and Astrophysics, The Pennsylvania State University, University Park, PA 16802, USA; kluhman@astro.psu.edu

<sup>3</sup> Center for Exoplanets and Habitable Worlds, The Pennsylvania State University, University Park, PA 16802, USA

<sup>4</sup> Kirkpatrick et al. (2014) also reported it as a high proper motion object in a later study.

were collected during the observations in February and July, respectively. The two reduced images are shown in Figure 1 with the previous epochs of *WISE* and *Spitzer* data from Luhman (2014b) for a  $1' \times 1'$  area surrounding WISE 0855–0714.

We have measured astrometry for WISE 0855–0714 in each of the four epochs of *Spitzer* data in the following manner, which produces more accurate results than the methods applied to the first two epochs by Luhman (2014b). Pixel coordinates were measured for all point sources in the corrected basic calibrated data (CBCD) versions of the individual [4.5] exposures using the Astronomical Point-source Extractor (APEX) Single Frame pipeline within the Mosaicking and Point-source Extraction software package (Makovoz & Marleau 2005). We applied a new distortion correction to those pixel coordinates that is more accurate than the one that is available from the *Spitzer* pipeline (T. Esplin, in preparation; see also Dupuy & Kraus 2013). The corrected coordinates for stars with  $S/N > 20$  and detections in more than two frames were used to compute relative offsets in  $x$ ,  $y$ , and rotation among the frames for a given epoch. We used the APEX multiframe pipeline to combine the registered CBCD images for each epoch and measure the positions of all detected sources. We identified all objects from the Point Source Catalog of the Two Micron All-Sky Survey (2MASS, Skrutskie et al. 2006) that were within  $2'$  of WISE 0855–0714, were not blended with other stars in the images from *Spitzer*, 2MASS, and *WISE*, and have proper motions of  $\lesssim 0''.02 \text{ yr}^{-1}$ , which resulted in a sample of 15 stars. We measured offsets in right ascension, declination, and rotation for that sample between 2MASS and the first *Spitzer* epoch and applied them to the source catalog from the latter to align it to the 2MASS astrometric system. The catalogs from the other *Spitzer* epochs were then aligned to the first epoch using stars that were within  $2'$  of WISE 0855–0714 and have  $[4.5] < 17$ . To characterize the errors in the astrometry for WISE 0855–0714, we first computed the differences in right ascension and declination between adjacent IRAC epochs for stars in a magnitude range encompassing WISE 0855–0714 ( $[4.5] = 13\text{--}16$ ). We then estimated the  $1\sigma$  errors based on two statistics, the median absolute deviation of those differences and the deviations from zero that contained 68% of the distribution. The astrometry for WISE 0855–0714 from each of the four *Spitzer* epochs is presented in Table 1.

### 3. WISE ASTROMETRY

In addition to the astrometry from *Spitzer*, we also make use of the detections of WISE 0855–0714 from *WISE* and *NEOWISE* when measuring its parallax. By comparing the *WISE* images to the first two epochs from *Spitzer*, Luhman (2014b) found that WISE 0855–0714 is blended with a group of background objects (primarily two sources with similar fluxes) in both epochs from *WISE* (see Figure 1). For each of the *WISE* epochs, Luhman (2014b) measured astrometry for the blend of WISE 0855–0714 and the contaminants from the coaddition of the single-exposure images at  $4.6 \mu\text{m}$  (denoted as *W2*), which is the *WISE* band in which WISE 0855–0714 dominates. Because WISE 0855–0714 had moved away from the background sources by the time of the *Spitzer* observations, Luhman (2014b) was

able to use the *Spitzer* images to estimate the true positions of WISE 0855–0714 in the *WISE* epochs in the following manner. For a grid of locations in a *Spitzer* image surrounding the *WISE* coordinates of WISE 0855–0714, he added an artificial star with the [4.5] flux of WISE 0855–0714, smoothed the image to the resolution of *WISE*, and measured astrometry for the blend of the artificial star and the background objects. For the simulated image in which the latter coordinates matched the astrometry measured for the blend in *WISE*, the artificial star’s inserted location was adopted as the true position of WISE 0855–0714. Wright et al. (2014) measured new astrometry for the blend of WISE 0855–0714 and its contaminants by applying software developed for the AllWISE Source Catalog to the *W2* images from each of the two *WISE* epochs. They also measured astrometry for the brown dwarf from *W2* images that were obtained in May of 2014 by *NEOWISE*. To account for the blending in the *WISE* images, Wright et al. (2014) included a parameter that related the true position to the observed position in their least-squares fitting of the proper motion and parallax.

For our analysis, we adopt the astrometry measured by Wright et al. (2014) for the blends of WISE 0855–0714 and the background sources in the two *WISE* epochs and for the brown dwarf alone in the *NEOWISE* epoch. To place those data on the same astrometric system as the *Spitzer* astrometry, we calculated the average differences in right ascension and declinations between 2MASS and AllWISE for the 15 2MASS reference stars from Section 2. The resulting offset of  $(0.1, 0'')$  was added to  $(\alpha, \delta)$  for each of the three epochs of astrometry from Wright et al. (2014). We are assuming that those data from Wright et al. (2014) are on the same astrometric system as the AllWISE Source Catalog. To correct the astrometry from *WISE* for the blended background sources, we applied the procedure from Luhman (2014b) that was summarized earlier in this section. For the errors in the corrected positions, we adopted the ranges in right ascensions and declinations of the inserted artificial stars that reproduced the errors in the observed, blended astrometry from Wright et al. (2014). We prefer the method of correcting the astrometry from Luhman (2014b) over the one from Wright et al. (2014) because the former makes use of the accurate astrometry and photometry of the contaminants that are available from *Spitzer*, which should comprise all of the information necessary for a reliable simulation of the blending. In addition, the fitting procedure from Wright et al. (2014) could produce erroneous results if astrometric perturbations from a companion are present. Table 1 contains the final astrometry that we adopt for WISE 0855–0714 from *WISE* and *NEOWISE*.

### 4. PARALLAX AND PROPER MOTION

#### 4.1. Previous Measurements

Two previous studies, Luhman (2014b) and Wright et al. (2014), have reported measurements of the proper motion ( $\mu$ ) and parallax ( $\pi$ ) of WISE 0855–0714. Based on the two epochs from *WISE* and the first two epochs from *Spitzer*, Luhman (2014b) arrived at  $(\mu_\alpha, \mu_\delta) = (-8.06 \pm 0.09, 0.70 \pm 0.07'' \text{ yr}^{-1})$  and  $\pi = 0.454 \pm 0.045''$ . Wright et al. (2014) added

a fifth epoch of astrometry from *NEOWISE*, measured new astrometry from the *WISE* epochs, and addressed the blending in the latter with an alternative method from that in Luhman (2014b), as discussed in Section 3. Combining those data with the *Spitzer* astrometry from Luhman (2014b), they derived  $(\mu_\alpha, \mu_\delta) = (-8.051 \pm 0.047, 0.657 \pm 0.050'' \text{ yr}^{-1})$  and  $\pi = 0.448 \pm 0.033''$ . Their errors in the proper motion and parallax were smaller than those from Luhman (2014b) because of the additional epoch from *NEOWISE* and the smaller errors for their *WISE* astrometry.

Wright et al. (2014) concluded that their analysis confirmed the results from Luhman (2014b). However, Wright et al. (2014) did not present new astrometry that was capable of accurately detecting a large parallax independently from the *Spitzer* images. Instead, rather than confirming the large parallax, their one additional epoch refined the proper motion, which in turn allowed the *Spitzer* data to slightly better constrain the parallax. Wright et al. (2014) also demonstrated that an alternative correction for the contamination of WISE 0855–0714 in the *WISE* images produces a similar proper motion and parallax as the correction method from Luhman (2014b).

#### 4.2. New Measurements

We applied least-squares fitting of proper and parallactic motion to the seven epochs of astrometry for WISE 0855–0714 in Table 1 with the IDL program MPFIT. The reduced  $\chi^2$  was fairly close to unity (0.5), indicating a good fit. We checked the errors from that procedure by creating 1000 sets of astrometry that consisted of the sum of the measured astrometry and Gaussian noise, and fitting parallactic and proper motion to each set. The resulting standard deviations of  $\mu_\alpha$  and  $\mu_\delta$  were similar to the errors from MPFIT. However, the standard deviation of the parallax was larger than the MPFIT error ( $0''.015$  vs.  $0''.013$ ); we have adopted the former for the parallax error. Our derived proper motion and parallax are presented in Table 2. They are consistent with the previous estimates from Luhman (2014b) and Wright et al. (2014). We show the relative coordinates among the seven epochs in Figure 2 after subtraction of the best-fit proper motion.

### 5. DISCUSSION

The original parallactic distance of  $2.20^{+0.24}_{-0.20}$  pc for WISE 0855–0714 (Luhman 2014b) was  $\sim 1 \sigma$  from the distances of WISE J104915.57–531906.1 AB ( $2.02 \pm 0.02$  pc, Boffin et al. 2014) and Wolf 359 ( $2.386 \pm 0.012$  pc, van Altena et al. 1995), which were the third and fourth closest systems to the Sun that were known prior to the discovery of WISE 0855–0714. Our measurement of  $2.31 \pm 0.08$  pc demonstrates more definitively that WISE 0855–0714 is likely the fourth closest known system. Among known Y dwarfs, WISE 0855–0714 is now roughly tied with WD 0806–661 B (Subasavage et al. 2009) for the smallest percentage error in its parallax ( $\sim 3$ –4%).

Luhman (2014b) estimated the effective temperature of WISE 0855–0714 by comparing  $M_{4.5}$  and a limit on  $J - [4.5]$  to the values predicted by atmospheric and evolutionary models of brown dwarfs. The selected models

were defined primarily by the following features: water clouds and chemical equilibrium (Burrows et al. 2003), cloudless and chemical equilibrium (Saumon et al. 2012), cloudless and non-equilibrium chemistry (Saumon et al. 2012), and 50% coverage of water, chloride, and sulfide clouds and chemical equilibrium (Morley et al. 2012, 2014). The latter three sets of atmospheric models utilize the evolutionary calculations of Saumon & Marley (2008). The cloudless models with equilibrium and non-equilibrium chemistry from Saumon et al. (2012) are the same as those used by Luhman et al. (2012) and Luhman (2014b). Cloudy models with non-equilibrium chemistry are also available (Morley et al. 2014), but they were not considered since they predict nearly identical photometry in  $J$  and  $[4.5]$  as the cloudy equilibrium models for the coldest Y dwarfs. When we repeat the temperature estimates from Luhman (2014b) using our parallax measurement and the  $J$ -band photometry from Faherty et al. (2014), we find that the new constraints on  $J - [4.5]$  and  $M_{4.5}$  imply temperatures of 225–280 K and 235–260 K, respectively, based on the four sets of models, and 225–240 K and 250–260 K for the models of Morley et al. (2014).

Previous studies have compared WISE 0855–0714 to other Y dwarfs and to theoretical models via color-magnitude diagrams (Luhman 2014b; Luhman et al. 2014; Faherty et al. 2014). In Figure 3, we show the positions of WISE 0855–0714 in diagrams of  $M_{4.5}$  versus  $J - [4.5]$  and  $M_{4.5}$  versus  $[3.6] - [4.5]$  based on our parallax measurement and photometry from Luhman (2014b) and Faherty et al. (2014) (see Table 2). We have selected  $[4.5]$  as the magnitude since it offers the smallest photometric errors among the filters in which WISE 0855–0714 and other Y dwarfs have been observed. For comparison, we have included in those diagrams data for known T and Y dwarfs with measured parallaxes and photometry in  $J$ ,  $[3.6]$ , and  $[4.5]$  (Cushing et al. 2011, 2014; Dupuy & Liu 2012; Tinney et al. 2012; Luhman et al. 2012, 2014; Beichman et al. 2013, 2014; Leggett et al. 2013; Marsh et al. 2013; Kirkpatrick et al. 2013; Dupuy & Kraus 2013)<sup>5</sup>. WISE 0855–0714 now has the best constraint on its position in  $M_{4.5}$  versus  $[3.6] - [4.5]$  among known Y dwarfs.

In addition to the data for T and Y dwarfs, we also plot in Figure 3 the magnitudes and colors predicted by three of the four sets of models described earlier. We have omitted the models of Burrows et al. (2003) since they differ the most from the data for WISE 0855–0714 (see Luhman et al. 2014). Among the remaining models, those using equilibrium and non-equilibrium chemistry are shown for temperatures of  $< 450$  K and  $< 350$  K, respectively. Except for WD 0806–661 B, the ages of the known Y dwarfs are unknown, so we have shown the model predictions for ages of 1, 3, and 10 Gyr, which span the ages of most stars in the solar neighborhood. As discussed previously (Leggett et al. 2010; Beichman et al. 2014; Luhman et al. 2014), these theoretical isochrones are significantly redder than the data for WISE 0855–0714 and other T and Y dwarfs in  $M_{4.5}$  versus  $[3.6] - [4.5]$ . In  $M_{4.5}$

<sup>5</sup> The uncertainty in the estimate of  $J$  for WD 0806–661 B from Luhman et al. (2014) is not well-determined, but we have adopted a value of 0.1 mag for Figure 3.

versus  $J - [4.5]$ , WISE 0855–0714 is  $1.5 \sigma$  bluer than the cloudless/chemical equilibrium models,  $2.5 \sigma$  redder than the cloudy models, and agrees with the cloudless/non-equilibrium models. For the Y dwarf sequence as a whole, no one set of models provides a clearly superior match.

In their analysis of a diagram of  $M_{W2}$  versus  $J - W2$ , which is analogous to  $M_{4.5}$  versus  $J - [4.5]$ , Faherty et al. (2014) found that WISE 0855–0714 was  $2.7 \sigma$  bluer than the cloudless/chemical equilibrium models from Saumon et al. (2012) and was within  $1 \sigma$  of the cloudy models from Morley et al. (2012, 2014), which they cited as the first evidence of water ice clouds outside the solar system. However, WISE 0855–0714 is closer to those cloudless models than the cloudy models in  $M_{4.5}$  versus  $J - [4.5]$ , as shown in Figure 3. Furthermore, in both  $M_{4.5}$  versus  $J - [4.5]$  and  $M_{W2}$  versus  $J - W2$ , the positions of WISE 0855–0714 are reproduced by the cloudless models from Saumon et al. (2012) that use non-equilibrium chemistry. Thus, those data do not serve as evidence

for or against the presence of water clouds. Nevertheless, WISE 0855–0714 is expected to contain such clouds given that they are predicted to form at  $T_{\text{eff}} < 400 \text{ K}$  (Burrows et al. 2003; Morley et al. 2014).

We acknowledge support from grant NNX12AI47G from the NASA Astrophysics Data Analysis Program. We thank Caroline Morley and Didier Saumon for providing their model calculations. *WISE* is a joint project of the University of California, Los Angeles, and the Jet Propulsion Laboratory (JPL)/California Institute of Technology (Caltech), funded by NASA. 2MASS is a joint project of the University of Massachusetts and the Infrared Processing and Analysis Center (IPAC) at Caltech, funded by NASA and the NSF. The Center for Exoplanets and Habitable Worlds is supported by the Pennsylvania State University, the Eberly College of Science, and the Pennsylvania Space Grant Consortium.

#### REFERENCES

- Andrei, A. H., Smart, R. L., Penna, J. L., et al. 2011, *AJ*, 141, 54  
 Beamin, J. C., Ivanov, V. D., Bayo, A., et al. 2014, *A&A*, submitted  
 Beichman, C., Gelino, C. R., Kirkpatrick, J. D., et al. 2013, *ApJ*, 764, 101  
 Beichman, C., Gelino, C. R., Kirkpatrick, J. D., et al. 2014, *ApJ*, 783, 68  
 Boffin, H. M. J., Pourbaix, D., Mužić, K., et al. 2014, *A&A*, 561, L4  
 Burrows, A., Sudarsky, D., & Lunine, J. I. 2003, *ApJ*, 596, 587  
 Cushing, M. C., Kirkpatrick, J. D., Gelino, C. R., et al. 2011, *ApJ*, 743, 50  
 Cushing, M. C., Kirkpatrick, J. D., Gelino, C. R., et al. 2014, *AJ*, 147, 113  
 Dahn, C. C., Harris, H. C., Vrba, F. J., et al. 2002, *AJ*, 124, 1170  
 Dupuy, T. J., & Kraus, A. L. 2013, *Science*, 341, 1492  
 Dupuy, T. J., & Liu, M. C. 2012, *ApJS*, 201, 19  
 Faherty, J. K., Burgasser, A. J., Walter, F. M., et al. *ApJ*, 752, 56  
 Faherty, J. K., Tinney, C. G., Skemer, A., & Monson, A. J. 2014, *ApJ*, 793, L16  
 Fazio, G. G., Hora, J. L., Allen, L. E., et al. 2004, *ApJS*, 154, 10  
 Kirkpatrick, J. D., Cushing, M. C., Gelino, C. R., et al. 2011, *ApJS*, 197, 19  
 Kirkpatrick, J. D., Cushing, M. C., Gelino, C. R., et al. 2013, *ApJ*, 776, 128  
 Kirkpatrick, J. D., Schneider, A., Fajardo-Acosta, S., et al. 2014, *ApJ*, 783, 122  
 Leggett, S. K., Burningham, B., Saumon, D., et al. 2010, *ApJ*, 710, 1627  
 Leggett, S. K., Morley, C. V., Marley, M. S., et al. 2013, *ApJ*, 763, 130  
 Luhman, K. L. 2013, *ApJ*, 767, L1  
 Luhman, K. L. 2014a, *ApJ*, 781, 4  
 Luhman, K. L. 2014b, *ApJ*, 786, L18  
 Luhman, K. L., Burgasser, A. J., Labbé, I., et al. 2012, *ApJ*, 744, 135  
 Luhman, K. L., Morley, C. V., Burgasser, A. J., Esplin, T. L., & Bochanski, J. J. 2014, *ApJ*, 794, 16  
 Mainzer, A., Bauer, J., Cutri, R. M., et al. 2014, *ApJ*, 792, 30  
 Makovoz, D., & Marleau, F. R. 2005, *PASP*, 117, 1113  
 Manjavacas, E., Goldman, B., Reffert, S., & Henning, T. 2013, *A&A*, 560, A52  
 Marocco, F., Smart, R. L., Jones, H. R. A., et al. 2010, *A&A*, 524, A38  
 Marsh, K. A., Wright, E. L., Kirkpatrick, J. D. et al. 2013, *ApJ*, 762, 119  
 Morley, C. V., Fortney, J. J., Marley, M. S., et al. 2012, *ApJ*, 756, 172  
 Morley, C. V., Marley, M. S., Fortney, J. J., et al. 2014, *ApJ*, 787, 78  
 Saumon, D., & Marley, M. S. 2008, *ApJ*, 689, 1327  
 Saumon, D., Marley, M. S., Abel, M., Frommhold, L., & Freedman, R. S. 2012, *ApJ*, 750, 74  
 Skrutskie, M., Cutri, R. M., Stiening, R., et al. 2006, *AJ*, 131, 1163  
 Smart, R. L., Tinney, C. G., Bucciarelli, B., et al. 2013, *MNRAS*, 433, 2054  
 Subasavage, J. P., Jao, W.-C., Henry, T. J., et al. 2009, *AJ*, 137, 4547  
 Tinney, C. G., Burgasser, A. J., & Kirkpatrick, J. D. 2003, *AJ*, 126, 975  
 Tinney, C. G., Faherty, J. K., Kirkpatrick, J. D., et al. 2012, *ApJ*, 759, 60  
 van Altena, W. F., Lee, J. T., & Hoffleit, E. D. 1995, *The General Catalogue of Trigonometric Stellar Parallaxes* (4th ed.; New Haven: Yale Univ. Obs.)  
 Vrba, F. J., Henden, A. A., Luginbuhl, C. B., et al. 2004, *AJ*, 127, 2948  
 Wang, Y., Jones, H. R. A., Smart, R. L., et al. 2014, *PASP*, 126, 15  
 Werner, M. W., Roellig, T. L., Low, F. J., et al. 2004, *ApJS*, 154, 1  
 Wolf, M. 1919, *Veroeffentlichungen der Badischen Sternwarte zu Heidelberg*, 7, 195  
 Wright, E. L., Eisenhardt, P. R. M., Mainzer, A. K., et al. 2010, *AJ*, 140, 1868  
 Wright, E. L., Mainzer, A., Kirkpatrick, J. D., et al. 2014, *AJ*, in press  
 Zapatero Osorio, M. R., Béjar, V. J. S., Miles-Páez, P., et al. 2014, *A&A*, 568, A6

TABLE 1  
ASTROMETRY FOR WISE J085510.83–071442.5

$\alpha$ (J2000) ( $^{\circ}$ )	$\sigma_{\alpha}$ ( $''$ )	$\delta$ (J2000) ( $^{\circ}$ )	$\sigma_{\delta}$ ( $''$ )	MJD	Source
133.7952573	0.125	−7.2450910	0.135	55320.4	<i>WISE</i>
133.7943232	0.133	−7.2450719	0.142	55511.3	<i>WISE</i>
133.7881873	0.028	−7.2445207	0.024	56464.5	<i>Spitzer</i>
133.7870881	0.028	−7.2444491	0.024	56677.3	<i>Spitzer</i>
133.7868488	0.028	−7.2444561	0.024	56712.3	<i>Spitzer</i>
133.7862461	0.158	−7.2442562	0.175	56782.4	<i>NEOWISE</i>
133.7858505	0.028	−7.2443176	0.024	56839.7	<i>Spitzer</i>

NOTE. — The *WISE* and *NEOWISE* data are from Wright et al. (2014) after the adjustments described in Section 3.

TABLE 2  
PARALLAX, PROPER MOTION, AND PHOTOMETRY FOR WISE J085510.83–071442.5

Parameter	Value	Reference
$\pi$	$0.433 \pm 0.015''$	1
$\mu_{\alpha} \cos \delta$	$-8.10 \pm 0.02'' \text{ yr}^{-1}$	1
$\mu_{\delta}$	$0.70 \pm 0.02'' \text{ yr}^{-1}$	1
$Y$	$> 24.4^a$	2
$J$	$25.0^{+0.53}_{-0.35}$	3
$H$	$> 22.7^a$	4
$K_s$	$> 18.6^a$	5
$W1$	$17.82 \pm 0.33$	4
$W2$	$14.02 \pm 0.05$	4
[3.6]	$17.44 \pm 0.05$	6
[4.5]	$13.89 \pm 0.02$	6

REFERENCES. — (1) this work; (2) Beamin et al. (2014); (3) Faherty et al. (2014); (4) Wright et al. (2014); (5) VISTA Hemisphere Survey; (6) Luhman (2014b).

<sup>a</sup> S/N < 3.

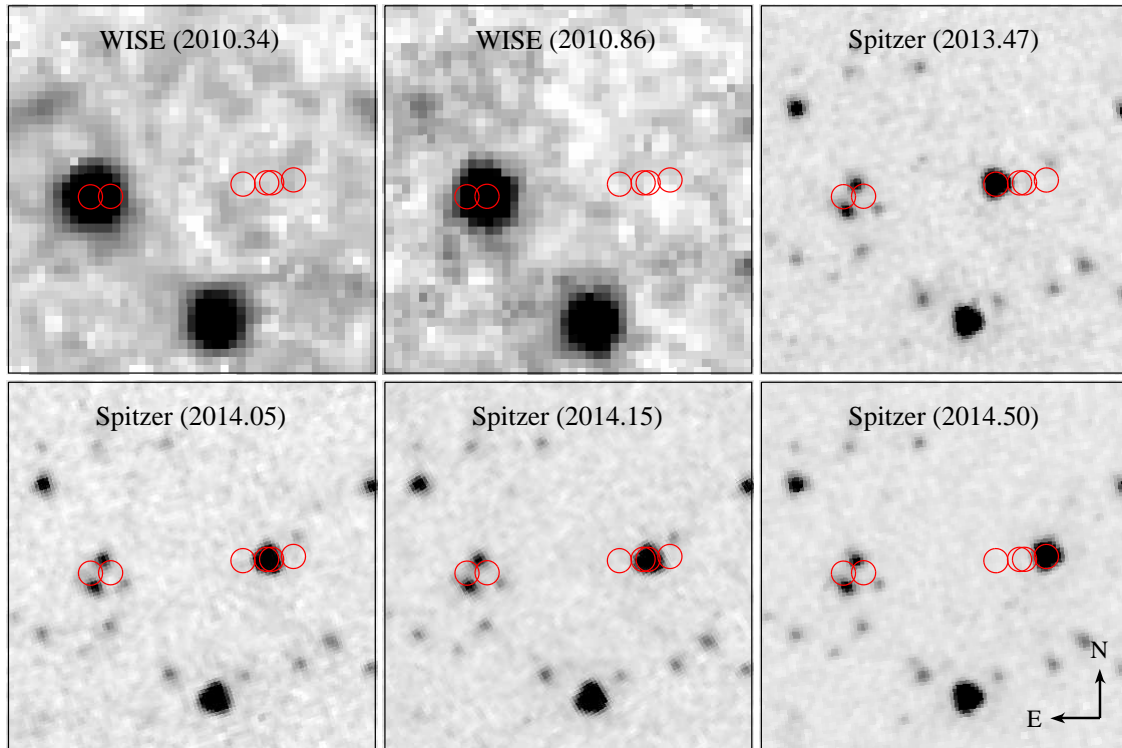


FIG. 1.— Images of WISE 0855–0714 from *WISE* ( $W2$ ) and *Spitzer* ( $[4.5]$ ). The first four images were presented by Luhman (2014b) and the latest two images were obtained in this work. The positions of WISE 0855–0714 are marked by the circles. The size of each image is  $1' \times 1'$ .

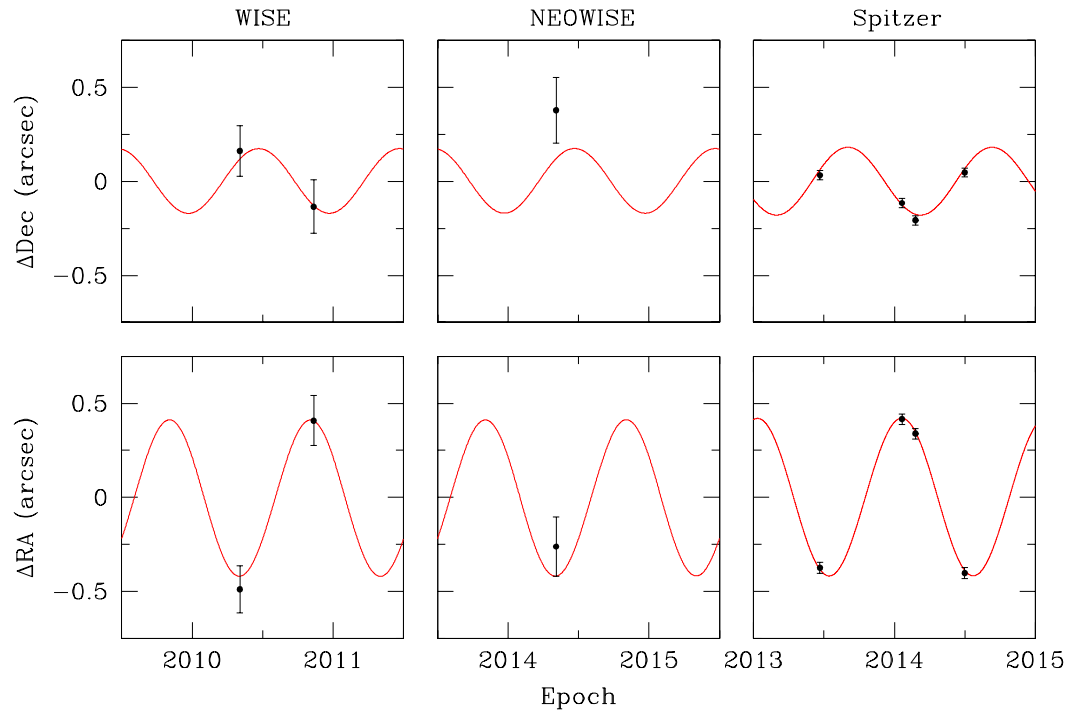


FIG. 2.— Relative astrometry of WISE 0855–0714 (Table 1) compared to the best-fit model of parallactic motion (Table 2, red curve). The proper motion produced by the fitting has been subtracted.

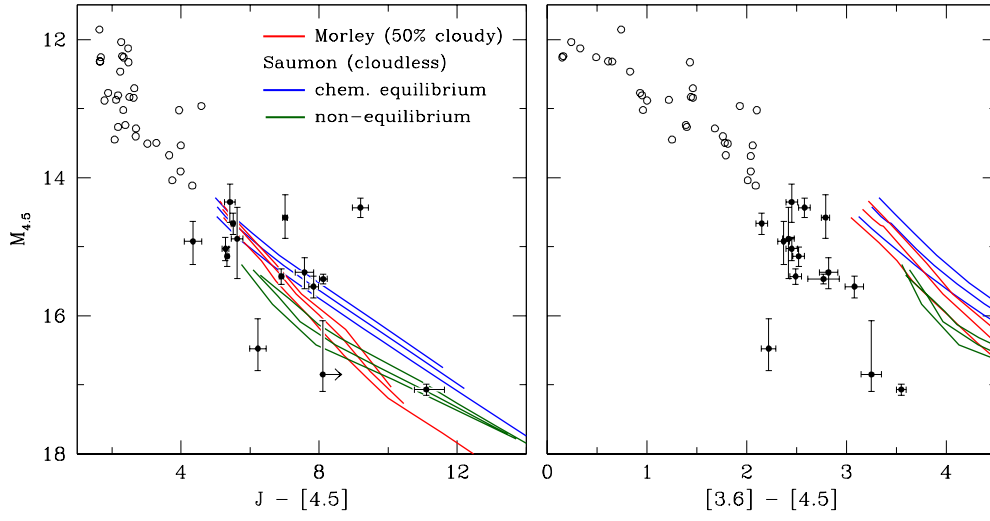


FIG. 3.— Color-magnitude diagrams for WISE 0855–0714 (faintest point, Luhman 2014b; Faherty et al. 2014, this work) and samples of T dwarfs (open circles, Dupuy & Liu 2012, references therein) and Y dwarfs (filled circles with error bars, Cushing et al. 2011, 2014; Tinney et al. 2012; Luhman et al. 2012, 2014; Beichman et al. 2013, 2014; Leggett et al. 2013; Marsh et al. 2013; Kirkpatrick et al. 2013; Dupuy & Kraus 2013). These data are compared to the magnitudes and colors predicted by theoretical models for ages of 1, 3, and 10 Gyr (solid lines, Saumon et al. 2012; Morley et al. 2012, 2014).